ISBN: 978-3-95450-247-9 ISSN: 2673-5490 doi: 10.18429/JACoW-IPAC2024-WEPR27

FLUKA SIMULATIONS OF NEUTRINO-INDUCED EFFECTIVE DOSE AT A MUON COLLIDER*

G. Lerner†, C. Ahdida, C. Carli, A. Lechner, J. M. Mańczak, A. Frasca [1‡],
CERN, Geneva, Switzerland
[1] also at the University of Liverpool, Liverpool, United Kingdom

Abstract

During the operation of a muon collider in an underground tunnel, most circulating muons decay into an electron (or positron) and a neutrino-antineutrino pair, resulting in a narrow disk of high-energy neutrinos emitted radially in the collider plane and emerging on the Earth's surface at distances of several km. Thus, dedicated studies are required to assess any potential radiation protection risks to the public due to the interaction of such neutrinos near the surface. This work presents a set of FLUKA Monte Carlo simulations aimed at characterizing the radiation showers generated by the interactions of high-energy neutrinos from TeV-scale muon decays in a reference sample of soil. The results are expressed in terms of effective dose in soil at different distances from the muon decay, quantifying the peak dose and the width of the radiation cone, for beam energies of 1.5 TeV and 5 TeV. The implications of these results for realistic muon collider scenarios are discussed, along with possible methods to mitigate the local neutrino flux.

INTRODUCTION

In high-energy muon colliders [1, 2], studied within the International Muon Collider Collaboration (IMCC) [3], the overwhelming majority of the injected muons are lost via the decays illustrated in Fig. 1. The muon decays generate dense neutrino cones in the forward direction (with a small angular width due to the $1/\gamma$ boost) that propagate through the underground soil and emerge on the Earth's surface [4–6]. For characteristic collider design and parameters [7], the decays in the arcs give rise to a radial disk of neutrinos in the collider plane, while more dense neutrino beams emerge from the straight sections due to subsequent muon decays in the same direction. Despite the low cross section, very high neutrino fluxes could result in measurable radiation levels beyond the boundaries of the laboratory, requiring dedicated mitigation efforts to reduce them to negligible levels. This paper examines the radiation showers generated by neutrino interactions in a reference soil sample (Table 1) with the FLUKA Monte Carlo code [8–10]. After reviewing the kinematic properties of the neutrinos and their interaction cross sections, FLUKA is used to evaluate the effective dose [11] produced by their interactions in soil. The material dependence of the dose is, instead, not covered.

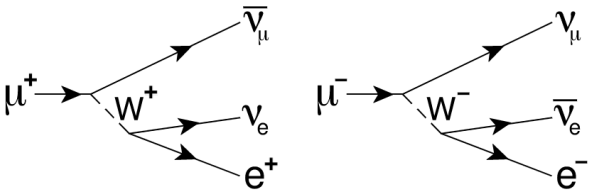

Figure 1: Positive and negative muon decay diagrams.

Table 1: Mass composition of the reference soil sample used in this paper, with a density of 2 g/cm^3.

Material	Mass %	Material	Mass %
Oxygen	50	Iron	1.4
Silicon	20	Potassium	1
Calcium	19.5	Hydrogen	0.6
Carbon	3	Magnesium	0.5
Aluminium	3	Sodium	0.01

MUON COLLIDER NEUTRINOS

The energy distribution of neutrinos and antineutrinos from the decay of 5-TeV muons is shown in Fig. 2, for all neutrino flavours and for the sub-sample of those interacting in soil. The latter distribution is obtained by applying an energy-dependent weight to the neutrinos, proportionally to their macroscopic interaction cross section in soil (Fig. 3) derived from the FLUKA neutrino library [12]. The spectrum of interacting neutrinos peaks at around half of the muon energy, and it is relatively harder for the muon flavour. From Figs. 2 and 3, one can compute the average macroscopic cross section of both flavours of neutrinos and antineutrinos from muon decays,

$$\Sigma_{\text{avg}} = \int \Sigma(E) \cdot \frac{dN}{dE} dE,$$

as presented in Table 2.

FLUKA SIMULATIONS

The macroscopic cross sections in Table 2 represent the average interaction probability of neutrinos per unit distance travelled in soil, and are used to normalize FLUKA simulations of the resulting radiation showers. Neutrino interactions can be sampled over layers of soil of arbitrary thickness at several km from the muon decay point, taking into account the energy and angular distributions of neutrinos from mono-directional and mono-energetic muon decays. The

* Funded by the European Union (EU). Views and opinions expressed are however those of the authors only and do not necessarily reflect those of the EU or European Research Executive Agency (REA). Neither the EU nor the REA can be held responsible for them. Work endorsed by IMCC.
† giuseppe.lerner@cern.ch
‡ Presenter

ISBN: 978-3-95450-247-9 ISSN: 2673-5490 doi: 10.18429/JACoW-IPAC2024-WEPR27

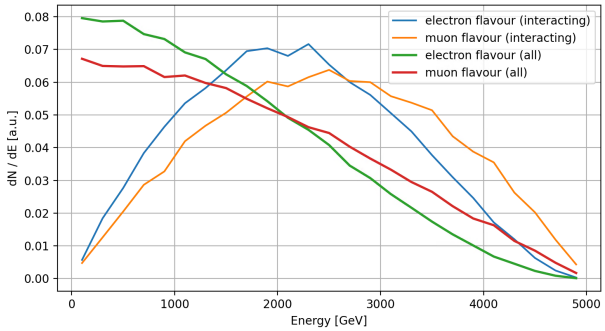

Figure 2: Energy distribution of all neutrinos and of neutrinos interacting in soil, obtained from FLUKA simulations of muon decays, normalized to unit integral.

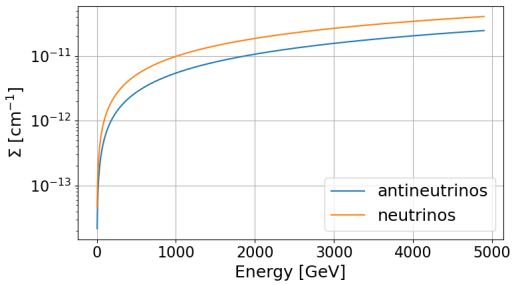

Figure 3: Macroscopic cross section of neutrinos and antineutrinos in soil as a function of their energy.

effective dose in soil is then computed as a function of the longitudinal distance z and the radial distance R from the trajectory axis of the muon decay.

To characterize the shower propagation, Fig. 4 shows the 2D (R-z) effective dose produced by electron neutrinos from 5-TeV mono-directional positive muons, sampling the interactions only in the final 10 m of soil at a 10 km from the decay (but similar figures can be made at other distances). The shower width is of the order of a few tens of cm, reflecting the small width of the neutrino cone. Figure 5 then shows the 1D projections of the effective dose as a function of z in the shower core for neutrinos from both positive and negative muons, proving that a plateau is reached a few meters after the first interaction. In turn, this implies that sampling neutrino interactions over few meters of soil is sufficient to reproduce realistic scenarios, where neutrino

Table 2: Average macroscopic cross section in soil of neutrinos from muon decays, obtained as the convolution between the energy distribution of the neutrinos (Fig. 2) and their macroscopic cross sections (Fig. 3).

	1.5 TeV	**5 TeV**	
$\Sigma^{\nu_e}_{\text{avg}}$ [cm^{-1}]	$4.56 \cdot 10^{-12}$	$1.39 \cdot 10^{-11}$	μ^+ decay
$\Sigma^{\bar{\nu}_\mu}_{\text{avg}}$ [cm^{-1}]	$2.87 \cdot 10^{-12}$	$9.22 \cdot 10^{-12}$	
$\Sigma^{\nu_\mu}_{\text{avg}}$ [cm^{-1}]	$5.27 \cdot 10^{-12}$	$1.60 \cdot 10^{-11}$	μ^- decay
$\Sigma^{\bar{\nu}_e}_{\text{avg}}$ [cm^{-1}]	$2.47 \cdot 10^{-12}$	$7.96 \cdot 10^{-12}$	

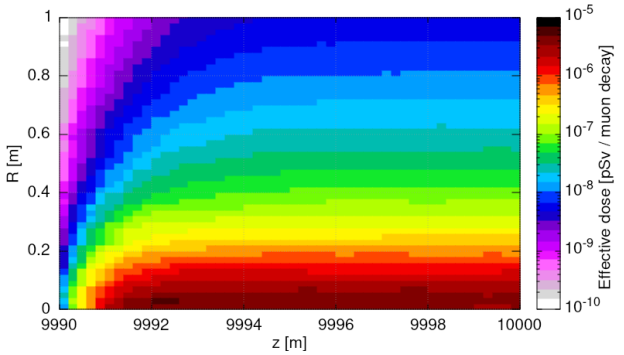

Figure 4: Effective dose build-up from electron neutrino interactions simulated with FLUKA in a 10 m thick layer of soil as a function of z and R at 10 km from the decay of 5-TeV positive muons.

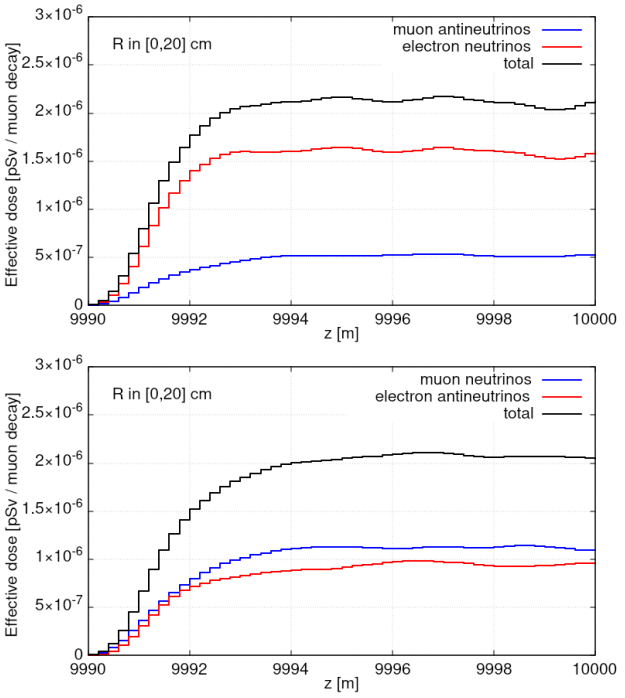

Figure 5: Effective dose build-up from neutrino interactions simulated with FLUKA in a 10 m thick layer of soil as a function of z at 10 km from the decay of 5-TeV positive (top) and negative (bottom) muons, for R in the $[0, 20]$ cm range.

beams interact uniformly along their km-long underground trajectories generating a uniform level of effective dose (with possible variations due to changes in soil density and composition). As shown in Fig. 6, the dose decreases rapidly when the neutrinos cross from the soil into air (at 90°), suggesting that the plateau dose in soil can be used as a conservative upper dose limit on the Earth's surface.

EFFECTIVE DOSE KERNELS

Having established that the effective dose reaches a plateau along the axis of the neutrino cone, it is useful to study the transverse dose profile, as shown in Fig. 7 for the case of positive muon decay products interacting at a baseline distance of 100 km. The distribution is fitted with a

ISBN: 978-3-95450-247-9 ISSN: 2673-5490 doi: 10.18429/JACoW-IPAC2024-WEPR27

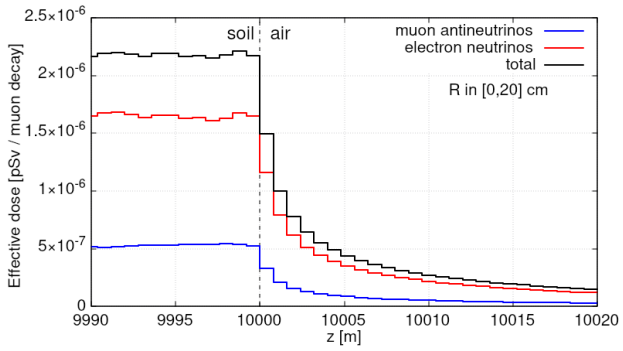

Figure 6: Effective dose from neutrino interactions from 5-TeV positive muon decays at the transition from soil to air.

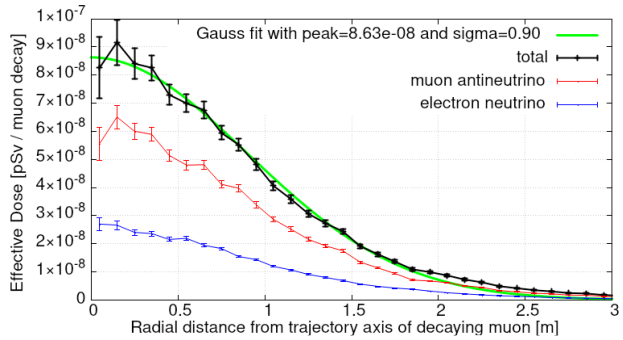

Figure 7: Radial profile of the effective dose in soil from neutrino interactions from 5-TeV positive muon decays, at 100 km from the muon decay point, with Monte Carlo errors.

Gaussian function parameterized by a peak effective dose and a width σ, which provides a good model of the curve with the exception of the tails (that are anyway only accounting for a negligible fraction of the dose). By repeating similar simulations and fits for neutrinos from positive and negative muon decays, and at different muon energies and baseline distances, we obtain the results in Table 3, which we refer to as the effective dose kernels in soil. These parameters, that are obtained from mono-directional muon decays, can be folded with muon trajectory distributions from specific portions of a muon collider to obtain more realistic, but still conservative dose models (see, e.g., Ref. [4]). Quantitatively, as shown in Fig. 8, the peak dose per muon decay is larger by almost two orders of magnitude for 5 TeV muons compared to 1.5 TeV ones, due to the higher neutrino cross section and the narrower neutrino cone. Instead, the width σ is larger for the 1.5 TeV case, as expected.

CONCLUSIONS

The operation of muon colliders leads to the emission of a high density disk of neutrinos in the collider plane, with particularly dense neutrino fluxes generated by the straight sections. Thorough studies of the resulting effective dose at the Earth's surface are needed to ensure that it remains negligible. The FLUKA simulations presented in this paper are aimed at characterizing the radiation showers emitted by the decay products of 1.5 TeV and 5 TeV muons in their simplest form, i.e., for mono-directional muons, but fully

Table 3: Effective dose kernel parameters of neutrino-induced radiation in soil for muon beam energies of 1.5 TeV (top) and 5 TeV (bottom).

1.5 TeV	**Peak eff. dose [pSv / decay]**		**σ [m]**	
	μ^-	μ^+	μ^-	μ^+
5 km	$2.09 \cdot 10^{-7}$	$2.19 \cdot 10^{-7}$	0.17	0.16
10 km	$6.57 \cdot 10^{-8}$	$6.56 \cdot 10^{-8}$	0.32	0.32
15 km	$3.28 \cdot 10^{-8}$	$3.34 \cdot 10^{-8}$	0.47	0.46
20 km	$1.98 \cdot 10^{-8}$	$1.99 \cdot 10^{-8}$	0.60	0.60
40 km	$5.42 \cdot 10^{-9}$	$5.49 \cdot 10^{-9}$	1.17	1.17
60 km	$2.53 \cdot 10^{-9}$	$2.51 \cdot 10^{-9}$	1.71	1.71
80 km	$1.44 \cdot 10^{-9}$	$1.42 \cdot 10^{-9}$	2.29	2.29
100 km	$9.20 \cdot 10^{-10}$	$9.21 \cdot 10^{-10}$	2.85	2.84

5 TeV	**Peak eff. dose [pSv / decay]**		**σ [m]**	
	μ^-	μ^+	μ^-	μ^+
5 km	$1.57 \cdot 10^{-5}$	$1.63 \cdot 10^{-5}$	0.05	0.05
10 km	$4.86 \cdot 10^{-6}$	$5.38 \cdot 10^{-6}$	0.10	0.10
15 km	$2.54 \cdot 10^{-6}$	$2.70 \cdot 10^{-6}$	0.15	0.14
20 km	$1.56 \cdot 10^{-6}$	$1.55 \cdot 10^{-6}$	0.19	0.20
40 km	$4.80 \cdot 10^{-7}$	$4.62 \cdot 10^{-7}$	0.37	0.38
60 km	$2.33 \cdot 10^{-7}$	$2.22 \cdot 10^{-7}$	0.54	0.55
80 km	$1.38 \cdot 10^{-7}$	$1.31 \cdot 10^{-7}$	0.71	0.73
100 km	$9.16 \cdot 10^{-8}$	$8.63 \cdot 10^{-8}$	0.87	0.90

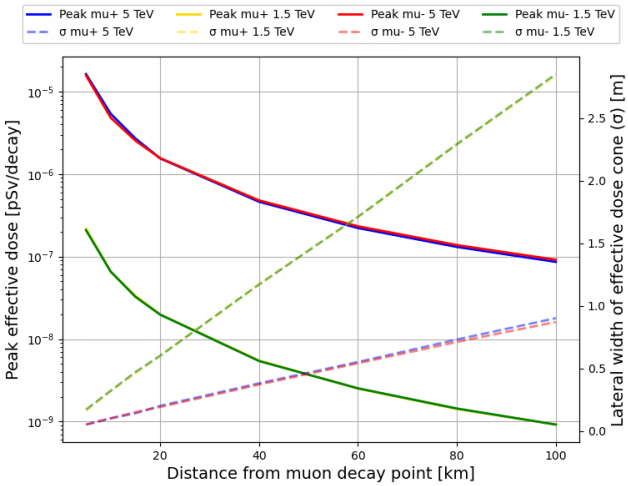

Figure 8: Effective dose kernel parameters of 1.5 TeV and 5 TeV muons in soil.

taking into account the distribution of neutrino energies and angles of emission. The main results are the effective dose kernel parameters in Table 3 and Fig. 8, that can serve as the basis for collider-specific calculations as the ones in Ref. [4]. Overall, the high peak effective dose values in the kernel (particularly at 5 TeV) imply that it is essential to fully consider the muon beam divergences when computing the dose in realistic scenarios. Dedicated measures to further spread the neutrino flux, such as beam wobbling techniques, are also examined.

ISBN: 978-3-95450-247-9 ISSN: 2673-5490 doi: 10.18429/JACoW-IPAC2024-WEPR27

REFERENCES

[1] H. A. Ali *et al.*, "The muon smasher's guide," 2022. doi:10.48550/arXiv.2103.14043

[2] J. P. Delahaye *et al.*, "Muon colliders," 2019. doi:10.48550/arXiv.1901.06150

[3] "International muon collider collaboration website," https://muoncollider.web.cern.ch.

[4] C. Carli *et al.*, "Neutrino generated radiation from a high energy muon collider," in *Proc. IPAC'23*, Venice, Italy, May 2023, pp. 925–928. doi:10.18429/JACoW-IPAC2023-MOPL166

[5] B. J. King, "Potential hazards from neutrino radiation at muon colliders," in *Proc. 1999 Particle Accelerator Conference*, New York City, NY, USA, vol. 1, Mar.-Apr. 1999, pp. 318–320. doi:10.1109/PAC.1999.795694

[6] N. Mokhov and A. V. Ginneken, "Neutrino radiation at muon colliders and storage rings," *J. Nucl. Sci. Tech.*, vol. 37, no. sup1, pp. 172–179, 2000. doi:10.1080/00223131.2000.10874869

[7] "MuCol project," https://muoncollider.web.cern.ch/node/262.

[8] "FLUKA.CERN website," https://fluka.cern.

[9] G. Battistoni *et al.*, "Overview of the FLUKA code," *Ann. Nucl. Energy*, vol. 82, pp. 10–18, 2015. doi:10.1016/j.anucene.2014.11.007

[10] C. Ahdida *et al.*, "New Capabilities of the FLUKA Multi-Purpose Code," *Front. Phys.*, vol. 9, p. 788 253, 2022. doi:10.3389/fphy.2021.788253

[11] D. Bozzato, R. Froeschl, "Implementation of ICRP116 Fluence to Effective Dose Conversion Coefficients in a FLUKA user routine," CERN, Tech. Rep. CERN-OPEN-2023-009, 2020. https://cds.cern.ch/record/2861988

[12] G. Battistoni, P. R. Sala, M. Lantz, A. Ferrari, and G. Smirnov, "Neutrino interactions with FLUKA," *Acta Phys. Pol. B*, vol. 40, pp. 2491–2505, 2009.